Ferromagnetic resonance studies of Ni nanowire arrays

U. Ebels,[1] J. -L. Duvail,[2] P. E. Wigen,[3] L. Piraux,[4] L. D. Buda,[1] and K. Ounadjela[1]
[1]*Institut de Physique et Chimie des Matériaux de Strasbourg, F-67037 Strasbourg, France*
[2]*Institut des Matériaux, 2 rue de la Houssinière, 44322 Nantes, France*
[3]*Department of Physics, Ohio State University, 174 West 18th Avenue, Columbus, Ohio 43210*
[4]*Unité de Physico-Chimie et de Physique des Matériaux, Place Croix du Sud 1, B-1348 Louvain-la-Neuve, Belgium*
(Received 2 March 2001; published 21 September 2001)

Using ferromagnetic resonance, the angular dependence of the uniform precession mode of infinite cylinders is investigated at room temperature for low density Ni nanowire arrays, embedded in a polycarbonate membrane, with wire diameters ranging from 35 nm to 500 nm. All wires reveal a very similar behavior of the resonance field vs angle, independent of the wire diameter and wire density, corresponding to the uniform precession mode of an infinite cylinder including the shape demagnetization anisotropy and a small uniaxial anisotropy contribution. From the analysis of the angular dependence of the linewidth, the distribution of the wire orientation and the effective anisotropy field can be estimated. The latter is broadened due to the presence of a sub-structure in the absorption spectra.

DOI: 10.1103/PhysRevB.64.144421 PACS number(s): 76.50.+g, 75.75.+a, 75.30.Gw

I. INTRODUCTION

In light of the increasing interest in using magnetic nanostructured materials for device applications, a complete understanding of their static and dynamic magnetic properties is required. Recently, much effort has been expended in analyzing the magnetization reversal process and the magnetic microstructure of Ni and Co nanowires grown by electrodeposition in track-etched polycarbonate membranes.[1–4] Nanowires of this type provide a versatile and reproducible system, suitable for studies of magnetization processes[1–4] as well as transport phenomena[5] in high aspect ratio cylindrical magnets (length 22 μm, diameters down to 30 nm). For such nanostructured materials it is possible to study both, a large ensemble of wires (more than 10^6) as well as isolated single wires. Although studies on single wires are crucial to understand the mechanism by which, e.g., the magnetization of a single wire reverses, it is also of importance for possible device applications to quantify the distribution of the internal fields for wire arrays containing a large number of wires.

The internal fields include the domain-wall nucleation field and the depinning field describing the reversal by wall propagation as well as the anisotropy field H_u. While it is possible to estimate the distribution of the nucleation and depinning fields from macroscopic hysteresis loops in combination with magnetic-force microscopy imaging,[4] dynamic techniques such as ferromagnetic resonance are conventionally used to characterize the distribution of the anisotropy field strength and its angular spread.[6] Recently, microwave stripline experiments on membranes containing Co, NiFe, and Ni nanowires with diameters of 120 nm revealed the possibility of observing the uniform resonance mode in these nanowire arrays.[7] Here, these measurements are extended to characterize the effective anisotropy field H_{eff} for ensembles of Ni nanowires with diameters ranging from 35 nm to 500 nm using conventional angular-dependent ferromagnetic resonance (FMR) at *Q* band (34.4 GHz) and at *K* band (23.6 GHz). Conventional FMR currently has still the advantage of yielding well-defined spectra from which a quantitative analysis of the angular dependence of the resonance fields and lineshapes can be obtained. Such a quantitative analysis is presented here for the linewidth taking into account the distribution of the wire orientation inside the membrane and the distribution of the effective magnetic anisotropy by calculating the field dependence of the susceptibility (at constant frequency) from the Landau-Lifschitz-Gilbert equation.[6]

II. EXPERIMENT

The Ni-wire arrays were prepared by the method of electrodeposition inside the pores of a polycarbonate membrane produced at the lab scale as described in Refs. 8,9. The individual Ni wires inside the array are randomly distributed and are aligned parallel to each other (within a deviation of up to $\pm 5°$). They have a length of 22 μm and are characterized by a cylindrical shape with a variation in diameter of less than 5% and with a low-surface roughness. Only wire arrays as a whole with several times of 10^6 wires inside a membrane were investigated. In Table I are summarized the corresponding wire diameters, wire densities, and average wire separations (as calculated from the densities assuming a closed-packed lattice). It is noted that for the densities chosen, the dipolar interaction between the wires are negligible. Such interactions have to be taken into account once the average distance approaches the wire diameter.[10]

Previous experiments on the magnetization reversal using alternating gradient-force magnetometry and superconducting quantum interference device magnetometry reveal that at room temperature the magnetic anisotropy is dominated by the shape anisotropy.[12] Thus the individual Ni wires can be considered as a model system for an infinite long cylinder. The saturation field values are typically below 2 kOe for cycling the applied field parallel to the wire axis and below 6 kOe for cycling the applied field perpendicular to the wire axis.[10]

In the room-temperature FMR experiments presented in the following, the microwave pumping field h_{rf} had a fre-

TABLE I. The g value, the effective anisotropy field $H_{eff}=H_u+2\pi M_s$ and the uniaxial anisotropy field $H_u=2K_u/M_s$ as deduced from a fit of the experimental data to Eq. (2) using a value of $M_s=485$ emu/cm^3. ϕ denotes the wire diameter and s denotes the average separation between wires calculated from the pore density for a closed-packed wire arrangement. ΔH_u denotes the distribution of the uniaxial anisotropy field over the wire array and $\Delta\theta_w$ the distribution of the orientation of the wires inside the membrane.

ϕ (nm)	density $1/(\mathrm{cm}^2)$	s (nm)	f (GHz)	g fit	H_{eff} fit (kOe)	H_u fit (kOe)	f (GHz)	g fit	H_{eff} fit (kOe)	H_U fit (kOe)	ΔH_u	$\Delta\Theta$
35	1.5×10^9	287	34.4	2.16	3.55	0.50	23.6	2.17	3.45	0.40	1200	3°
70	2.4×10^8	697					23.6	2.15	3.55	0.50		
80	1.5×10^9	287	34.4	2.15	3.30	0.25	23.6	2.13	3.35	0.30		
270	6.9×10^6	4090	34.4	2.18	3.35	0.30	23.6	2.19	3.35	0.30	1500	3°
500	6.9×10^6	4090	34.4				23.6	2.19	3.20	0.15	1100	5°

quency of either $f=34.4$ GHz (Q band) or $f=23.6$ GHz (K band) and was always oriented perpendicular to the applied bias field H_o and to the wire axes, see Fig. 1. Before each field sweep, the Ni wires were first saturated parallel to the wire axis and the field was subsequently reduced to zero. The angle θ_H of the applied bias field H_o was then changed in zero field such that H_o varied between parallel to the wire axis ($\theta_H=0°$) and perpendicular to the wire axis ($\theta_H=90°$), as indicated in Fig. 1. The spectra were subsequently taken upon sweeping H_o.

III. RESULTS

A. Resonance Field

A typical sequence of FMR derivative spectra at $f=34.4$ GHz as a function of θ_H is shown in Fig. 2(a) for an ensemble of Ni wires with a diameter of 270 nm. One broad absorption peak is apparent. In all cases the resonance field of the absorption peak increases upon changing the angle from parallel (0°) to perpendicular (90°) to the wire axis that is in accordance with the wire axis being the effective magnetic easy axis. This sequence of FMR derivative spectra is similar for all wire diameters measured, with almost the same minimum and maximum resonance-field values, indicating very similar internal effective fields. The dependence of the resonance field H_{res} vs θ_H is shown in Fig. 3 for the diameters of 35 nm, 80 nm, and 270 nm (full dots, open dots, and square points, the curves are offset vertically by 1 kOe with respect to each other). The error bars for the determination of the resonance field is equivalent to the size of the points.

This angular dependence of H_{res} is fit to the uniform mode of an infinite cylinder with an effective uniaxial anisotropy (parallel to the wire axis) given by the shape demagnetization energy πM_s^2 and a small second-order uniaxial anisotropy contribution K_u. The corresponding energy expression is

$$E=(K_u+\pi M_s^2)\sin^2\theta-M_sH_o[\sin\theta\sin\theta_H\cos(\phi-\phi_H)+\cos\theta\cos\theta_H], \quad (1)$$

with (θ,ϕ) and (θ_H,ϕ_H) the polar and azimuthal angles of the magnetization M and the applied bias field H_o respectively. For $\phi=\phi_H=0$ this leads to the frequency-field dispersion:

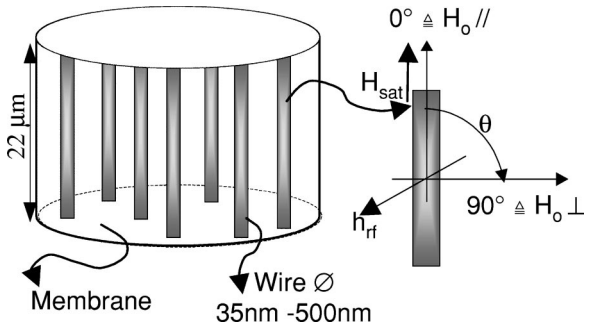

FIG. 1. A schematic, showing the random arrangement of the Ni wires inside the polycarbonate membrane and the orientation of the saturation field H_{sat}, the applied bias field H_o, and the microwave pumping field h_{rf}.

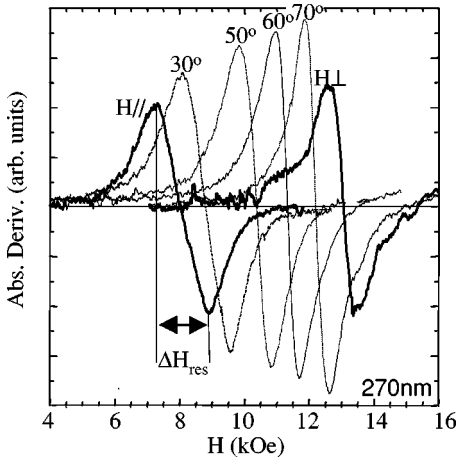

FIG. 2. A sequence of FMR derivative spectra for a 270-nm Ni-wire array at 34.4 GHz. The bias field varies between parallel $H\|$ to perpendicular $H\perp$ to the wire axis. The linewidth ΔH_{res} is indicated.

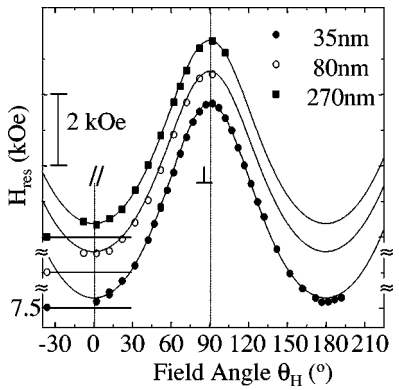

FIG. 3. The experimentally determined angular variation of the resonance field H_{res} at $f=34.4$ GHz, for three different wire arrays having diameters of 35 nm (full squares), 80 nm (open squares) and 270 nm (full circles). The different data set are offset vertically by 1 kOe with respect to each other, with the horizontal bar denoting 7.5 kOe for each spectrum. The full lines are fits of the data to Eq. (2) and the fit parameters are summarized in Table I.

$$\frac{\omega}{\gamma}=[\{H_{eff}\cos 2\theta_o+H_o\cos(\theta_o-\theta_H)\}\times\{H_{eff}\cos^2\theta_o+H_o\cos(\theta_o-\theta_H)\}]^{1/2}, \qquad (2)$$

with $H_{eff}=H_u+2\pi M_s$, $H_u=2K_u/M_s$ the anisotropy field and γ the gyromagnetic ratio $\gamma=g\mu_b/\hbar$ (μ_b = Bohr magnetic moment). The angle θ_o corresponds to the equilibrium angle of the magnetization, determined from the condition $dE/d\theta = 0$ for each field angle θ_H at the corresponding resonance field H_{res}.

The best fit of the data to Eq. (2) upon variation of H_{eff} and the g factor is shown in Fig. 3 by the solid lines for the different wire diameters. They describe well the measured angular dependence of H_{res} of the Ni-wire ensembles. It is noted, that fits including a fourth-order uniaxial anisotropy are less good and such terms have therefore not been considered further. The fit values are summarized in Table I. The fitted g value is slightly smaller than the value of $g=2.19$ listed in Ref. 11 for bulk Ni. The fitted effective field H_{eff} has an average value of 3.4 kOe that is slightly larger than the demagnetization field $H_d=2\pi M_s=3.05$ kOe when using the bulk value of the saturation magnetization $M_s=485$ emu/cm^3. This deviation is found for all wire-ensembles measured, with no systematic dependence on the wire diameter and is larger than can be explained by error bars. It would correspond to a 10% enhancement of the saturation magnetization, which is not considered as very likely. Therefore the deviation is attributed to a small additional second-order uniaxial anisotropy contribution H_u whose origin remains to be elucidated. However, it can be noted that from previous measurements[12] a slight texture of the polycrystalline Ni was found with the crystalline [110] axis aligned parallel to the wire axis. Considering the projection of the bulk-cubic anisotropy (with its easy axes along [111] and having a value of $H_u=200$ Oe)[13] onto the [110] axis, may yield some contributions, but cannot explain the full amount of H_u. Other contributions may arise through magneto-elastic effects induced by the membrane, similar to those found in earlier studies at low temperature.[12] For example, the value of $H_u=400$ Oe would correspond to a contraction of the lattice constant of 0.1% with respect to the bulk lattice value. This is at the limit of the accuracy with which a shift in the lattice constant can be determined from x-ray diffraction spectra for such polycrystalline nanowire arrays, compare Ref. 12.

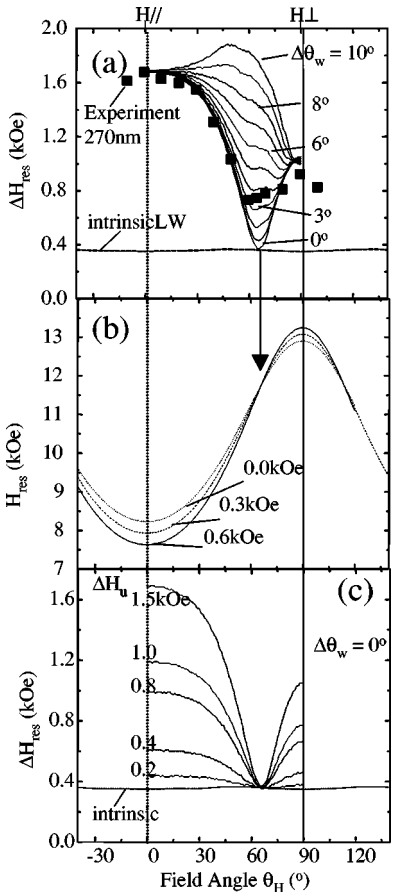

FIG. 4. (a) The experimentally determined angular variation of the resonance-field linewidth $\Delta H_{res}(\theta_H)$ for the 270-nm wire array (full squares) as well as the calculated linewidths $\Delta H_{res}(\theta_H)$ (full lines) for different values of the wire orientation distribution $\Delta\theta_w=0°$ to 10° (in steps of 1°). Here the frequency is $f=34.4$ GHz, the g value is $g=2.19$, the uniaxial anisotropy field is $H_u=0.3$ kOe, and the uniaxial anisotropy field distribution $\Delta H_u=1.5$ kOe. The (almost) horizontal line is the calculated intrinsic linewidth. (b) The calculated angular variation of the resonance field H_{res} for three different uniaxial anisotropy values: 0 kOe (dotted), 0.3 kOe (dashed), and 0.6 kOe (full line). (c) The calculated angular dependence of ΔH_{res} for different distributions of the anisotropy $\Delta H_u=0.2$ kOe to 1.5 kOe and for $\Delta\theta_w=0$.

B. Linewidth

The linewidth ΔH_{res} was determined from the field separation of the maximum and minimum in the derivative absorption spectra, as indicated in Fig. 2. Its angular variation $\Delta H_{res}(\theta_H)$ is shown in Fig. 4(a) by the square dots for the 270-nm wire-ensemble measured at 34.4 GHz. It shows an

oscillatory behavior with a maximum at 0° and 90° and a minimum between 60° and 70°.

From theory, there are two important contributions to the linewidth ΔH_{res}.[11,14,15]

$$\Delta H_{res} = \Delta H_o + \Delta H_{inh} = \Delta H_o + \left|\frac{\partial H_{res}}{\partial H_{eff}}\right| \Delta H_{eff} + \left|\frac{\partial H_{res}}{\partial \theta_H}\right| \Delta\theta_H . \quad (3)$$

The first term of Eq. (3) is the intrinsic contribution ΔH_o, due to a viscous damping of the magnetization precession, while the second term ΔH_{inh} is due to inhomogeneities in the internal fields ΔH_{eff} and the wire orientation $\Delta\theta_H$.

The intrinsic contribution can be estimated using the bulk values for: the Gilbert damping parameter G (2.45×10^8 s^{-1}),[11] the g value (2.19),[11] and the saturation magnetization M_s (485 emu/cm^3). This yields for the Ni wires an average value of $\Delta H_o = 0.36$ kOe (0.26 kOe) at Q band (K band) that varies only by a few tens of Oersteds as a function of the field angle. This value is indicated in Fig. 4(a) by the (almost) horizontal line. Although the intrinsic damping is non-negligible, it is too low to explain the measured values and the angular dependence of ΔH_{res}. Therefore sample inhomogeneities corresponding to the second and third term of Eq. (3) must have a dominant contribution.

The wires are to a good approximation magnetically independent (low-wire density) and in consequence the measured resonance absorption is the integral of the absorption peaks of all individual wires. The linewidth then reflects the distribution of the parameters of the individual wires that vary in their exact orientation inside the membrane as well as in their value of the effective anisotropy field H_{eff}.

Distribution of H_{eff}. Assuming that the saturation magnetization and hence the demagnetization field is constant, the variation of the effective anisotropy field is given by the distribution of the magnetic anisotropy field $\Delta H_{eff} = \Delta H_u$. In Fig. 4(b) the angular variation of the resonance field H_{res} is shown for three different values of the magnetic anisotropy field (34.4 GHz and $g = 2.18$). It can be seen that upon increasing H_u, the resonance field at 0° decreases, but increases at 90°. Hence, the $H_{res}(\theta_H)$ curves all cross at some intermediate angle resulting in a minimum of $\Delta H_{res}(\theta_H)$ as also observed in Fig. 4(a) for the 270-nm wire ensemble.[6] Since ΔH_u vanishes at the minimum, but ΔH_{res} itself is still by 0.36 kOe larger than the intrinsic linewidth, there will be a contribution from the wire misorientation as well.

Distribution of H_{eff} *and of* θ_H. In order to evaluate more quantitatively the angular variation of the linewidth, the Landau-Lifshitz-Gilbert equation[6] was first solved in the small-angle approximation for an individual wire. From this the susceptibility and the absorbed power are calculated as a function of the bias field H_o for different field angles θ_H, yielding a theoretical absorption-derivative field sweep, similar to those shown in Fig. 2. The total absorbed power is given by the weighted integral over all wires, using a Gaussian distribution for the magnetic anisotropy field (standard deviation $2\sigma = \Delta H_u$) around the average value of H_u. The linewidth is then obtained from the calculated absorption-derivative field sweep in analogy to the experiment, Fig. 2. Typical results of the angular dependence of the linewidth ΔH_{res} for several values of ΔH_u and for $\Delta\theta_H = 0$ (zero wire misorientation) are shown in Fig. 4(c) ($g = 2.18$, $f = 34.4$ GHz, and $H_u = 0.3$ kOe) revealing a minimum at 65° with a corresponding minimum value given by the intrinsic linewidth.

Since the effective anisotropy of an individual wire has axial symmetry, the misorientation of the wires inside the membrane from the 0° position corresponds to an effective misorientation of the applied field angle θ_H, compare Fig. 1. To take this misorientation into account, the absorbed power-field sweeps are once more integrated over θ_H using a top-hat distribution function ($\theta_H \pm \Delta\theta_w$). A result is shown in Fig. 4(a) for $\Delta\theta_w$ varying between 0° and 10° in steps of 1° for $\Delta H_u = 1.5$ kOe (and $f = 34.4$ GHz, $g = 2.19$, $H_u = 0.3$ kOe).

From this calculated evolution, two interesting points are noted. First, the intermediate minimum at 65° develops into a maximum for increasing $\Delta\theta_w$. Accordingly, the presence of a minimum in the angular dependence of the linewidth indicates that the distribution of the (effective) magnetic anisotropy field dominates whereas the presence of a maximum indicates that a distribution of the wire misorientation dominates. Second, the linewidth values at 0° and 90° are unaffected by the distribution of the wire angle $\Delta\theta_w$ allowing for an independent determination of both distributions. Hence, using the calculation described above, the distribution ΔH_u can be fit to the values at 0° and 90° and the angle spread $\Delta\theta_w$ can be fit to the region around the minimum angle, since here ΔH_u is negligible.

Using this procedure, see Fig. 4(a), the values for the 270-nm Ni-wire array are obtained as $\Delta H_u = 1.5$ kOe ± 0.1 kOe and $\Delta\theta_w = 3.5° \pm 0.5°$. The parameters determined for other samples are given in Table I.

IV. DISCUSSION

While the value of $\Delta\theta_w$ is in accordance with those determined from structural characterization,[5] the distribution of the magnetic anisotropy ΔH_u appears to be rather large in comparison to the average value of H_u (0.3 kOe for 270 nm). This will be discussed in the following. A closer look at the spectra reveals a substructure in the absorption derivative scans with a shoulder on either the low- or the high-field side of the main peak. In Fig. 5, Q band spectra are shown for Ni nanowire arrays of different diameter at parallel resonance (0°), where the peak positions are indicated by the arrows. From the angular dependence of the resonance fields and the corresponding linewidths, two kinds of angular-dependent evolutions of the substructure can be distinguished for the different wire arrays: Type I corresponding to the behavior of the 270-nm wire array and Type II corresponding to the behavior of the 80-nm wire array described below.

For the 270-nm wire array, the substructure is not strongly pronounced at Q band, see Figs. 2 and 5. However at K band, a weak high-field peak is visible, as shown in Fig. 6(a), with

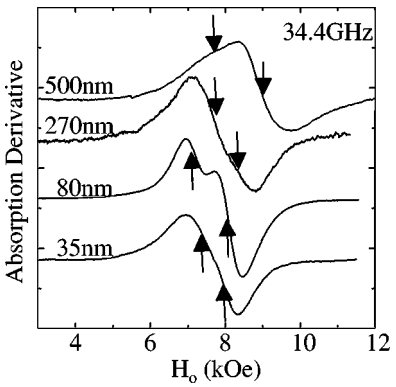

FIG. 5. *Q* band (34.4 GHz) absorption derivative spectra at 0° for Ni nanowire arrays of different diameter as indicated in the Figure. The arrows indicate the approximate position of the resonance fields for the different absorption peaks.

the estimated angular dependence of the peak positions given in Fig. 6(b). The field separation diminishes from 0.6 kOe at 0° and both peaks merge above 40°. Both peaks can be fit to the uniform mode described by Eqs. (1) and (2) by a reasonable set of (g,H_u) values.

While this behavior is quite similar for the smaller (35 nm) and larger diameters (270 nm and 500 nm), the behavior seems to be somewhat different for intermediate diameters of 80 nm. Here a clear double-peak structure is visible. In Fig. 7 the corresponding angular dependence of the absorption derivative spectra is shown for the 80 nm diameter Ni-wire array at $f=23.6$ GHz, together with the angular dependence of the peak-position H_{res} [inset (a)] and the linewidth ΔH_{res} [inset (b)]. The low-field peak appears to stay on the low-field side and cannot be fit by a reasonable set of (g,H_u) values, while the high-field peak is fit by the values given in Table I. It is also noted that the high-field peak is of stronger intensity than the low-field peak, although from the spectra in Fig. 7 it may appear to be the reverse. A deconvolution of both peaks using the derivative of two Lorentzian-lineshapes confirms that the high-field peak is 1.9 times stronger. A similar behavior was found for arrays with wire diameters of 70 nm and 120 nm.

The origin of these substructures needs further investigations. However, in order to exclude experimental ambiguities

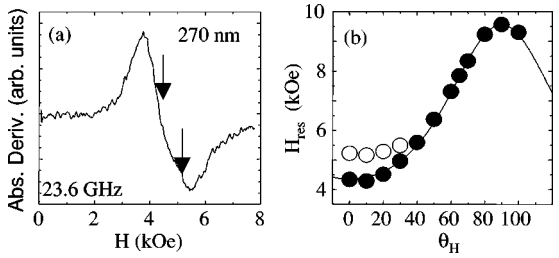

FIG. 6. (a) The $H\|$ (0°) absorption derivative spectrum and (b) the angular dependence of the resonance fields for the 270-nm Ni array at *K* band (23.6 GHz). The arrows in (a) indicate the approximate position of the resonance fields for the two absorption peaks. The open symbols in (b) correspond to the (weaker) high-field mode and the closed symbols to the (stronger) low-field mode.

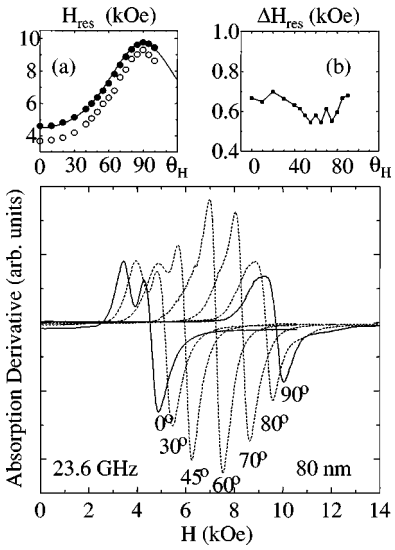

FIG. 7. The absorption derivative spectra for a 80-nm Ni array at *K* band (23.6 GHz) as a function of the applied field orientation θ_H. Inset (a) shows the corresponding resonance fields vs θ_H and inset (b) the corresponding measured linewidth vs θ_H. The open symbols in (a) correspond to the low-field mode and the closed symbols to the high-field mode.

it is noted that: (1) an inhomogeneity of the pumping field is excluded, since the spectra are the same for the same sample measured at *K* band and at *Q* band. While the $(3\ \mathrm{mm})^2$ samples used are about the size of the *Q*-band cavity, they are much smaller with respect to the larger *K*-band cavity. (2) A misalignment or bending of part of the sample is excluded. Such a misalignment would produce a larger resonance field at 0° and a smaller H_{res} at 90°. For the high-field peak of Fig. 6(b), the 0° value would then correspond to a misorientation of 30°. Such a strong bending of parts of the sample has not been observed and is also not consistent with the spread of the wire orientation inside the membrane.

In conclusion it can be said that for the Type I spectra Figs. 2 and 6, the existence of the substructure explains the broad combined linewidth given in Fig. 4(a). Both peaks are in agreement with the uniform FMR mode of an infinite cylinder containing a uniaxial anisotropy parallel to the wire axis and will therefore give rise to a minimum around 60–70° of the angular dependence of the combined linewidth.

In contrast, for the double-peak structure of the Ni-wire arrays of 80 nm diameter, only the high-field mode is consistent with the uniform mode of an infinite cylinder. The evolution of the linewidth and the line intensity of the absorption derivative of this high-field mode as a function of θ_H is characteristic for a wire ensemble with a distribution in the effective anisotropy field. This is evident from the negative part of the absorption derivative of the high-field peak shown in Fig. 7, where the lines become narrow and intense with a maximum around 60°. From this negative part, the linewidth is estimated and shown in the top-right inset. The value at 0° is lower than the corresponding one of the 270 nm array and a weak minimum around 60° is present. Regarding the low-field peak, further investigations are needed

to elucidate its origin. It is mentioned though, that recent calculations by Arias and Mills[16] have shown the possibility of exciting exchange/dipole spin-wave modes in these type of nanowires in the intermediate diameter range around 100 nm for the case that a surface anisotropy is present. This corresponds to the diameter range where in the experiments here a pronounced double-peak structure has been observed. This makes the system very exciting for future investigations.

V. SUMMARY

In summary, the angular dependence of the uniform ferromagnetic resonance mode and its linewidth were investigated for a series of low density, noninteracting nanowires, fabricated by electrodeposition inside the pores of a polycarbonate membrane. For all wire-diameters measured, a fit of the resonance-field position H_{res} vs the bias field angle θ_H yields an average g value of 2.17 and an effective anisotropy field of $H_{eff}=3.4$ kOe. This value is slightly larger than the demagnetization field of an infinite cylinder $2\pi M_s$ (using $M_s=485$ emu/cm^3) and indicates a small uniaxial anisotropy contribution oriented parallel to the wire axis. The analysis of the angular variation of the linewidth in terms of a distribution of this uniaxial magnetic anisotropy ΔH_u as well as a distribution of the wire orientation inside the membrane $\Delta\theta_w$ shows that the two contributions can be fit separately to the experimental data. For the wires investigated, this yields a maximum distribution of the wire orientation of $\pm 3.5°$ in agreement with structural investigations. In contrast the estimated distribution of the anisotropy field of ΔH_u is rather large in comparison to the average value of H_u and results from the presence of a substructure in the absorption derivative spectra. This substructure makes the system very exciting from a fundamental point of view. Its understanding will also be of importance for possible applications of such nanowire arrays as microwave devices.

ACKNOWLEDGMENTS

The authors wish to thank R. Legras and E. Ferain for providing the polycarbonate membrane samples used in this work. Furthermore the authors acknowledge R. Arias and D. L. Mills for interesting discussions and for providing their manuscript prior to publication. Finally, the authors would like to thank P. Molinié for using the FMR apparatus at the Institut des Matériaux (Nantes) where part of the measurements were carried out. L.P. is a Research Associate of the National Fund for Scientific Research (Belgium). This work was partly supported by the EC-TMR program ''Dynaspin'' (No. FMRX-CT97-0124) and the EC-Growth and Sustainable program ''NanoPTT'' (No. G5RD-CT1999-00135) as well as by the Belgian Interuniversity Attraction Pole Program (PAI-IUAP P4/10).

[1] W. Wernsdorfer, B. Doudin, D. Mailly, K. Hasselbach, A. Benoit, J. Meier, J.-Ph. Ansermet, and B. Barbara, Phys. Rev. Lett. **77**, 1873 (1996).
[2] J.-E. Wegrowe, D. Kelly, A. Franck, S.E. Gilbert, and J.-Ph. Ansermet, Phys. Rev. Lett. **82**, 3681 (1999).
[3] S. Pignard, G. Goglio, A. Radulescu, L. Piraux, and J.-L. Duvail, J. Appl. Phys. **87**, 824 (2000).
[4] Y. Henry *et al.* (unpublished).
[5] For a review, see A. Fert and L. Piraux, J. Magn. Magn. Mater. **200**, 338 (2000).
[6] J.F. Cochran, J.M. Rudd, M. From, B. Heinrich, W. Bennett, W. Schwarzacher, and W.F. Egelhoff, Phys. Rev. B **45**, 4676 (1992).
[7] G. Goglio, S. Pignard, A. Radulescu, and L. Piraux, Appl. Phys. Lett. **75**, 1769 (1999).
[8] T.M. Whitney, J.S. Young, P. Searson, and C. Chien, Science **261**, 1316 (1993).
[9] L. Piraux, J.M. George, J.F. Despres, C. Leroy, E. Ferain, R. Legras, K. Ounadjela, and A. Fert, Appl. Phys. Lett. **65**, 2484 (1994).
[10] A. Encinas, M. Demand, L. Piraux, I. Huyen, and U. Ebels, Phys. Rev. B **63**, 104415 (2001).
[11] M. Farle, Rep. Prog. Phys. **61**, 755 (1998); G. Dewar, B. Heinrich, and J.F. Cochran, Can. J. Phys. **55**, 821 (1977).
[12] S. Dubois, J. Colin, J.L. Duvail, L. Piraux, and A. Declémy, Phys. Rev. B **61**, 14 315 (2000).
[13] X. Buschow, in *Ferromagnetic Materials: A Handbook on the Properties of Magnetically Ordered Substances*, edited by E. P. Wohlfarth (North-Holland Publishing, Amsterdam, 1980).
[14] C. Chappert, K. Le Dang, P. Beauvillain, H. Hurdequint, and D. Renard, Phys. Rev. B **34**, 3192 (1986).
[15] W. Platow, A.N. Anisimov, G.L. Dunifer, M. Farle, and K. Baberschke, Phys. Rev. B **58**, 5611 (1998).
[16] R. Arias and D.L. Mills, Phys. Rev. B **63**, 134439 (2001)